JCRS

Journal of Chemical Reactivity and Synthesis 2021: 11(4) 228-243

Research Article

DFT studies of the hydroquinone adsorption on polypyrrole

Mozafar Rezaee*, Shahrbanoo Rahaman Setayesh

Department of Chemistry, Sharif University of Technology, Tehran, Iran

ARTICLE INFO:

Received:
30 September 2021

Accepted:
1 December 2021

Available online:
7 December 2021

✉: M. Rezaee
mozirezaee73@gmail.com

ABSTRACT

In this study, the adsorption hydroquinone on polypyrrole (ppy) adsorbents has been investigated using the density functional theory (DFT) method. Calculations were performed at two levels, b3lyp/6-31+G(d,p) and WB97XD/6-31+G(d,p). Studies were in the gas phase and water solvent with the conductive polarizable continuum model (CPCM) model. Evaluation of energy level changes of Homo and Lumo orbitals, hardness, softness, electrophilicity, dipole moment, charge transfer by Mulliken method and natural bonding orbitals, adsorption energy, density of states diagrams, molecular electrostatic potential, intermolecular distances and non-covalent interaction analysis has been performed.

Keywords: Adsorption; hydroquinone; Polypyrrole; Density functional theory (DFT).

1. Introduction

Phenolic compounds are one of the most widely used and abundant classes of ionizable organic acid compounds [1]. their high solubility in water and carcinogenic properties make them one of the most hazardous compounds for the environment. Phenolic compounds are the prerequisites and raw materials for the production of many drugs and industrial materials, so these materials are present in many industrial effluents such as petrochemical, pharmaceutical

and textile, and pesticides [2-4]. Most Environmental Protection agencies (EPA) have listed phenolic compounds and their derivatives as hazardous and harmful to humans and the environment. The united states environmental protection agency (USEPA), the Central Pollution Control board (CPCB), and the European Union (EU) set the standard amount for phenol and aniline in industrial and agricultural effluents, at 1.0 mg/L [5-7]. These substances can be transmitted to the human body and other organisms through respiration, skin, and drinking water. Exposure to phenolic compounds can damage organs such as the kidneys, spleen, and pancreas. Causes poisoning and disorders of the gastrointestinal tract, lung disorders, and even seizures [8]. For this reason, phenolic compounds are among the most dangerous compounds for humans, other living organisms, and the environment, so the need to eliminate these compounds is increasingly felt. Many studies have been done on adsorption phenolic compounds in theory [9-16]. Conductive polymers such as polypyrrole, polyaniline, and polythiophene have recently received much attention for their use as adsorbents due to their good adsorption, easy preparation, low cost for preparation, and suitable mechanical and chemical properties. [17-31]. These conductive polymers have also recently been widely used in drug delivery systems [32], fuel cells [33], and sensors [34]. In this work, the adsorption of hydroquinone on ppy using the density functional theory (DFT) at two levels of B3LYP/6-31+G (d,p) and WB97XD/6-31+G (d,p) was investigated. In this study The lowest molecular orbital energy (LUMO), the hig hest molecular orbital energy (HOMO), band gap (E_g), dipole moment (μ_d), reactivity parameters including chemical potential (μ), hardness (η), electrophilicity (ω) and softness (σ), adsorption energy (E_{ads}), minimum distance Between adsorbent and adsorbates (d), charge transfer by natural population analysis (Q_{NBO}) and Mulliken charge analysis ($Q_{mulliken}$), the density of states (DOS), molecular electrostatic potential (MEP), and non-covalent interaction analysis (NCI) were analyzed. The effect of solvent for adsorption on charged polypyrrole was studied by a Conductor polarizable-

continuum model (CPCM) which showed that the solvent leads the adsorption energy to more positive values.

2. Computational method

All calculations were performed using Gaussian 09 software package. The output files of the molecules were analyzed using the GaussView 06 software. Calculations were performed in gas phases at level B3LYP/6-31+G (d,p) [35] and WB97XD/6-31+G (d,p) [36,37] level of theory. Solvent phase with water solvent was investigated using a continuously polarized conductor model (CPCM). The energy of lowest unoccupied molecular orbital (LUMO), the energy of highest occupied molecular orbital (HOMO), band gap (Eg), moment dipole (μ), adsorption energy (E_{ads}), charge transfer by natural population analysis (NBO), and Mulliken analysis, minimum distance Between adsorbent and adsorbates (d), analysis of the density of states (DOS) and molecular electrostatic potential (MEP) was performed. Non-covalent interaction (NCI) analysis was performed to investigate the nature of intermolecular interactions at the level of the theory mentioned above using multiwfn and VMD software. GaussSum 3.0 was used to plot the density of states. A set of symbols is used to distinguish between optimized structures. for structures in the water solvent phase, sw is added to the end of each structure. For example, hydroquinonesw, meaning hydroquinone, is optimized in an aqueous solvent. To perform calculations at the level ofwb97xd/631+G (d, p) a w is added to the end of each structure, and not using it means calculating at the level of b3lyp.

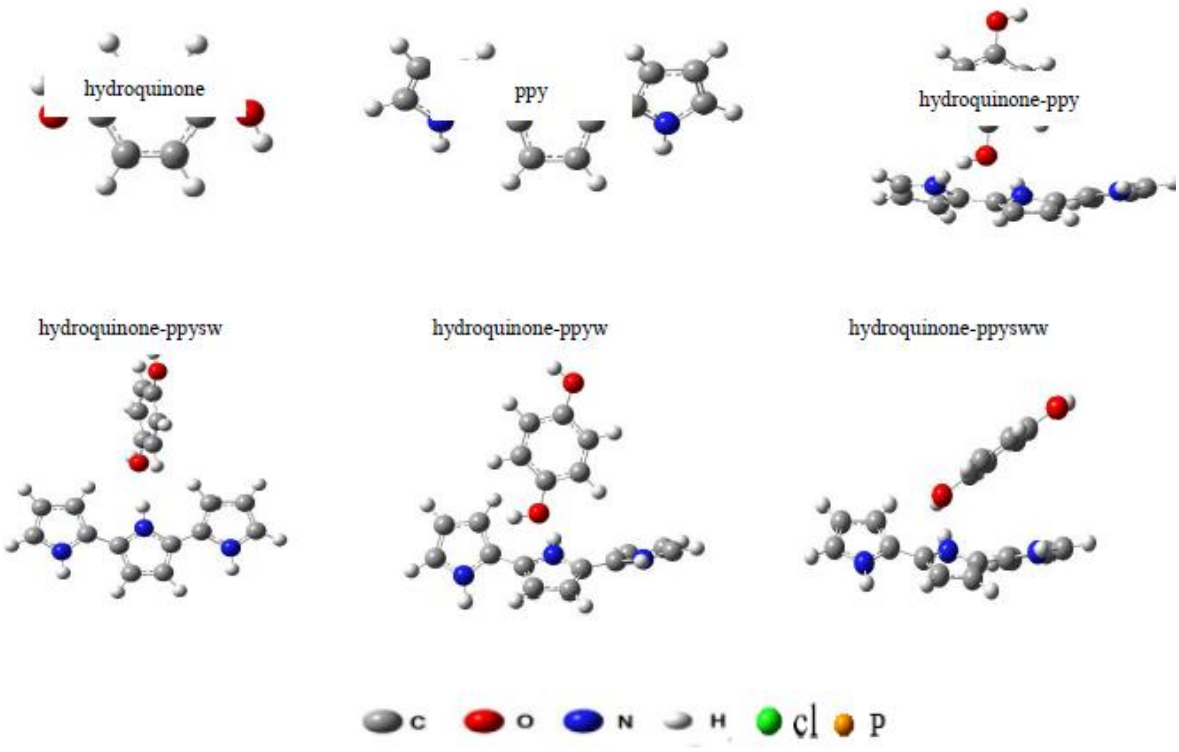

Fig. 1. The optimized structure of the hydroquinon and ppy, at B3LYP/6-31+G (d,p) level of theory in the gas phase. Adsorption of hydroquinone on ppy in gas and water phase at B3LYP/6-31+G (d,p)and WB97XD/6-31+G (d,p) level of theory.

The adsorption energies E_{ads} between adsorbates (phenolic compound) and adsorbents were obtained from the following equation:

$$\boldsymbol{E_{ads} = E(adsorbent - adsorbate) - E(adsorbent) + E(adsorbate)} \quad (\mathbf{1})$$

Where $E(adsorbent - adsorbate)$ is related to the energy of the adsorbent (ppy)-adsorbate (hydroquinone) complex. E (adsorbent) is the energy of polypyrrole as the adsorbent and E (adsorbate) is the energy of the hydroquinone.

The charge transfer between the adsorbent and the adsorbent during adsorption is obtained by the difference between the polypyrrole adsorbent charge before and after adsorption by the following equation

$$\Delta q = q_{ppy\ before\ adsorption} - q_{ppy\ after\ adsorption} \quad (2)$$

where $q_{ppy\ before\ adsorption}$ and $q_{ppy\ after\ adsorption}$ are total structure charges of the ppy before and after adsorption, respectively. We computed the electrophilicity index (ω). This index indicates the direction of charge transfer. A higher value of ω indicates the higher electrophilic power of the structure [38].

$$\omega = \frac{\mu^2}{2\eta} \quad (3)$$

$$\mu = \frac{(E_{HOMO} + E_{LUMO})}{2} \quad (4)$$

$$\eta = \frac{(-E_{HOMO} + E_{LUMO})}{2} \quad (5)$$

Where μ is electronic chemical potential, and η is the chemical hardness of the ground state [39-42].

3. Result and discussion

3.1. Optimized structure

The optimized structure of hydroquinone and ppy in the gas phase at B3LYP/6-31+G (d,p) level of theory, and adsorption of the hydroquinone on ppy at B3LYP/6-31+G (d,p) and WB97XD/6-31+G (d,p) level of theory in the gas phase and water solvent illustrated in Fig 1. We used three pyrrole monomers for polypyrrole.

3.2. intermolecular distances and dipole moment

In adsorption of hydroquinone on ppy The intermolecular distance is defined here as the minimum distance between the oxygen in the OH group and the hydrogen atoms attached to the nitrogen in the ppy adsorbent (Table 2). The indicated distances are in the range of intermolecular forces and physical absorption. In the case of dipole moments, the dipole moment in the solvent is generally greater than the gaseous phase due to the induction of an electric field by the solvent in the molecule. For the hydroquinone, the dipole moment is

small, which is due to the specific symmetry of the molecule, which means that the two substitutions of the hydroquinone molecules are similar. dipole moment is less in the wb97xd correlation-exchange function, which means less charge separation, and this can be a measure of stability. The change in the moment dipole of the adsorbent-adsorbed complex compared to isolated adsorbent and adsorbent indicates an interaction.

3.3. Molecular electrostatic potential (MEP)

Molecular electrostatic potential (MEP) gives important information than reactive electrophilic and nucleophilic sites. MEP surfaces of the hydroquinone and adsorption of the hydroquinone on these adsorbents were calculated and illustrated in Fig. 2. MEP was calculated for hydroquinone from $-3.045e^{-2}\ a.u.$ to $-3.045e^{+2}\ a.u.$ These potentials are often identified by a color scheme. Red indicates the most negative potential values and blue indicates the most positive potential values. The results show that the oxygen atom of the hydroquinone has a higher electron density (negative) and a red color [43]. This suggests that these groups may be considered nuclear attack sites. In contrast, ppy amine functional groups lead to high positive electron density. This indicates that amine groups are the electrophilic attack sites for ppy. MEP was calculated for polypyrrole from $-2.700e^{-2}\ a.u.$ to $+2.700e^{-2}\ a.u.$ According to these results, the mechanism of adsorption of hydroquinone on ppy can be done through electron density transfers between nuclear and electrophilic groups of adsorbents and adsorbates. In general, at the wb97xd correlation-exchange function for hydroquinone adsorption structures on polypyrrole, there is better interaction between electrophilic and nucleophilic groups compared to level b3lyp correlation-exchange function, which leads to more negative adsorption energy in this function. MEP was calculated for adsorption of the hydroquinone on polypyrrole from $-3.045e^{-2}$ a.u. to $+3.045e^{-2}\ a.u.$

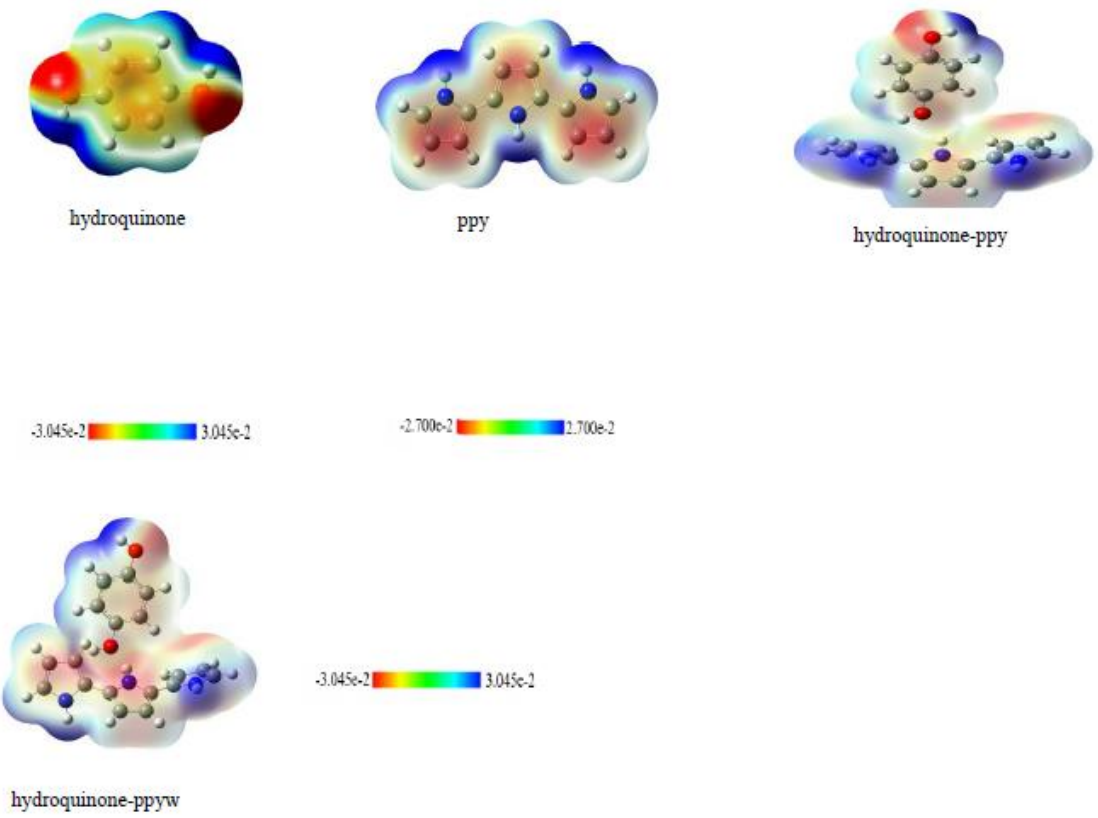

Fig. 2. MEP surfaces hydroquinone, ppy, in the gas phase at B3LYP/6-31G(d) level and adsorption of hydroquinone on ppy at b3lyp and wb97xd functional in thr gas phase.

3.4. natural bond orbital analysis (NBO)

Electron charge transfer was investigated by NBO and Mulliken methods. Electron charge transfer is defined as the difference between the absorbent charge before and after absorption. NBO analysis is more accurate than the Mulliken method [44] because Mulliken arbitrarily divides electrons between base functions and ignores electronegative and hybridizing effects as well as Pauli effects. NBO is the eigen state of the density matrix operator. Table 2 shows the charge transfer of adsorption of the hydroquinone on ppy. Transfer charges often indicate physical absorption. Transfer size is a measure of adsorption power. In the solvent phase, due to the electric field created in the solvent molecules and the charge transfer to the molecules, the charge transfer is higher than in the gas phase. In general, the higher the charge transfer, the more negative the absorption energy. For example, it can be seen that for most cases, the charge transfer in the correlation-exchange function of the wb97xd is greater than the b3lyp

and its adsorption energy is also higher. The difference in the size and sign of the charge transfer in the two methods of Mulliken and NBO is due to their different formalism in charge calculation.

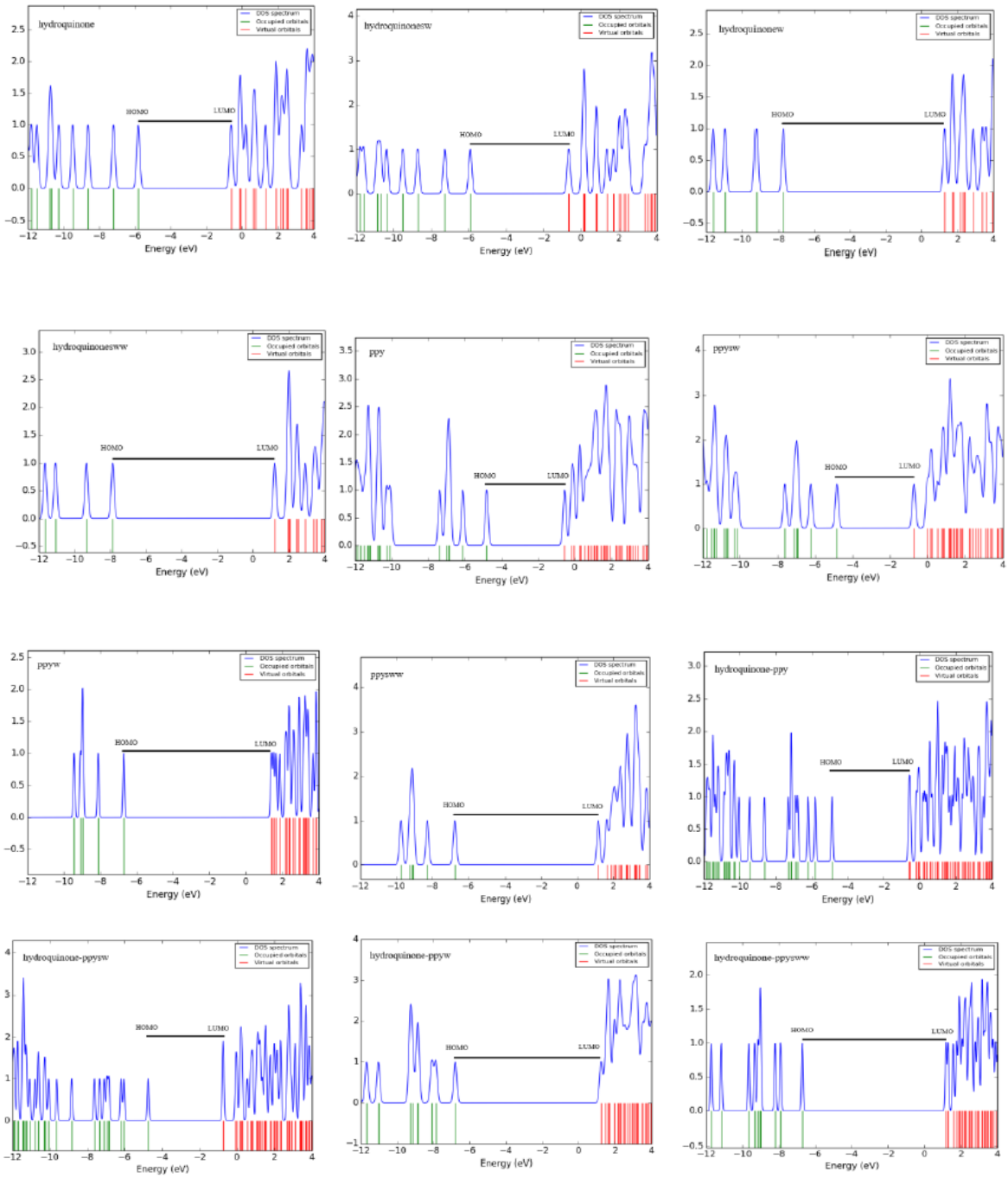

Fig. 3. DOS diagrams of isolated adsorbate in gas phase and solvent water at two levels of theory, ppy in gas and solvent phase at b3lyp and wb97xd functional, adsotption of hydroquinone on ppy in the gas phase, and water solvent at b3lyp and wb97xd functional

3.5. natural bond orbital analysis (NBO)

For understanding the electronic properties of structures, DOS was calculated for the isolated adsorbents and adsorbate and adsorbate-adsorbent complexes [45]. Figure 4 shows the dos diagrams, and the LUMO and HOMO energy levels are marked on them. Changes in HOMO and LUMO energy levels in the complex compared to adsorbents and isolated adsorbates indicate interaction. More bandgap makes greater kinetic stability. The bandgap in the wb97xd correlation exchange function is greater for the corresponding structures than the b3lyp correlation exchange function. This is in agreement with the more negative energy absorption in this exchange-correlation function. Mirror symmetry (Coulson-Rashbrook rule) is observed for orbitals [46].

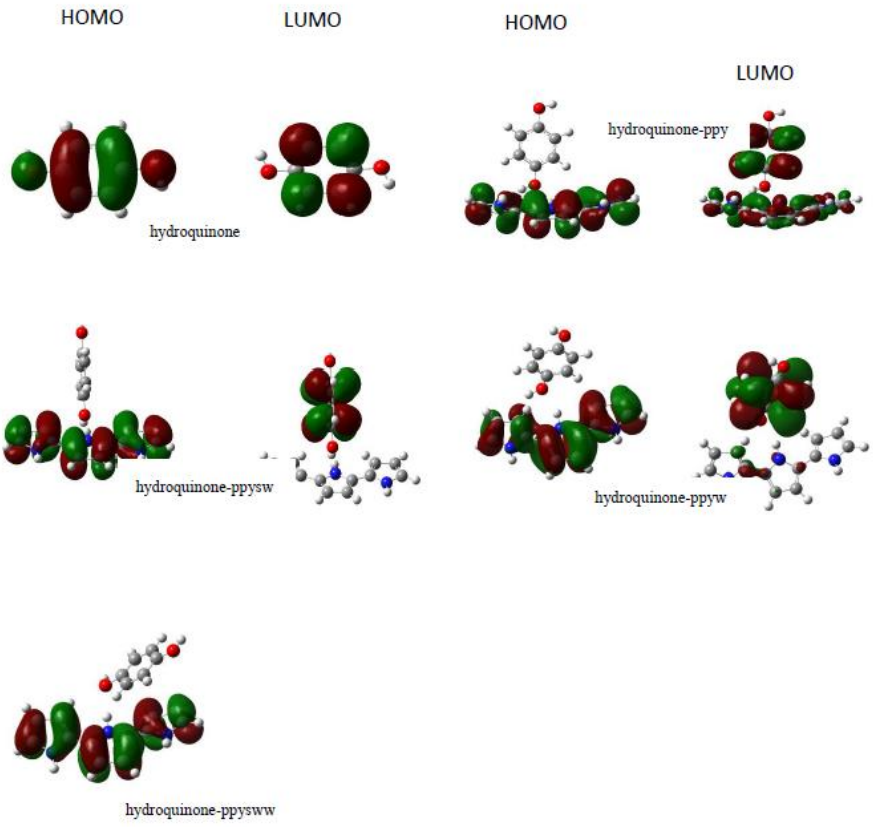

Fig. 4. LUMO and HOMO energy levels

3.6. Non-covalent interaction (NCI) analysis

Non-covalent interactions are a method used to understand the nature of the intermolecular force involved between molecules. The NCI indices rely on the electron density and the reduced density gradient (s), as shown in equation

$$s = \frac{1}{2(3\pi^2)^{\frac{1}{3}}} \frac{\nabla\rho}{\rho^{\frac{4}{3}}} \qquad (6)$$

This analysis can be used to determine intermolecular forces such as hydrogen bonding, van der Waals interactions, and repulsive steric interactions. Usually, two methods are used to make this analysis. In the first method, a graph is used that is generated with the plots of the reduced density gradient (s) versus (sign λ_2)ρ, where (sign λ_2)ρ is the electron density multiplied by the sign of the second Hessian eigenvalue (λ_2). The value of (sign λ_2)ρ is useful to predict the nature of interaction [47]. In the second method, intermolecular interactions in the NCI method can be visualized by gradient isosurface in the real space of the molecules. In the 3D visualization of NCI isosurface, Green color is used for van der Waals interaction, Blue color for hydrogen bonding, red color is used for repulsive steric interactions. Fig 5 shows NCI analysis. We used the second method in this project. To investigate intermolecular interactions and use non-covalent interaction analysis, adsorption of hydroquinone on polypyrrole. For the adsorption of hydroquinone on the ppy in the wb97xd functional, the van der Waals interaction and hydrogen bonding are greater than the other function.

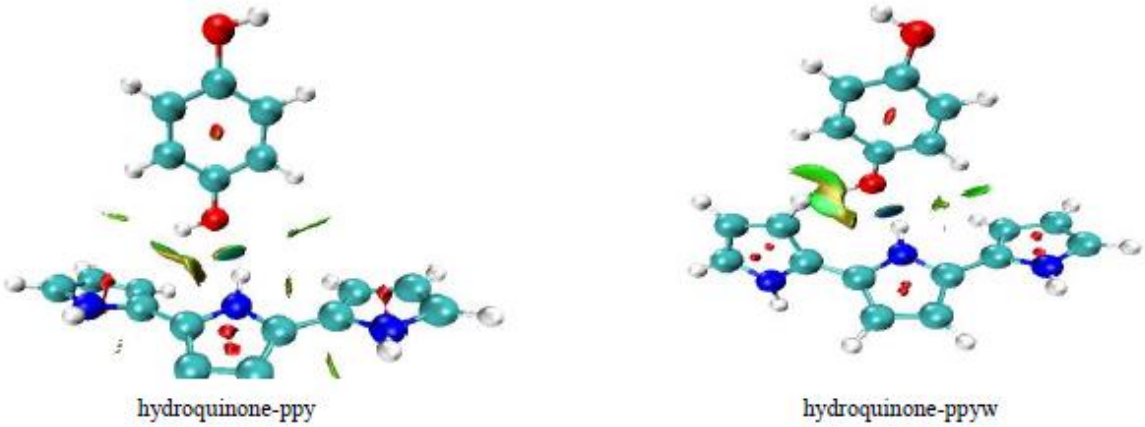

Fig. 5. Reduced density gradient isosurfaces are depicting non-covalent interaction (NCI) regions for adsorption of hydroquinone on ppy at b3lyp and wb97xd functional. The isosurfaces were constructed with RDG 0.5 au. The colors scaling from -0. 04 < (sign λ_2)ρ < 0.02 au.

3.7. Adsorption energy

In the calculations performed in this project, the adsorption energy in the gas phase is more negative than the solvent phase, and this is probably due to the lack of rotation of molecules in the solvent phase and the lack of a suitable optimized structure. Also, the adsorption energy for the correlation-exchange function wb97xd is more negative than b3lyp. The reason for this is the specific formalism of these correlation-exchange functions, which, as we saw in NCI analysis, the wb97xd functional involve intermolecular forces well and leads to appropriate optimized structures.

Table 1. The energy of the HOMO (E_{HOMO}) and LUMO (E_{LUMO}) orbitals, band gap energy (E_g), Dipole moment (μ_d), and for hydroquinone in phase gas and water solvent at B3LYP/6-31+G (d,p) and WB97XD/6-31+G(d,p) level of theory, ppy adsorbent and adsorption energy (E_{ads}) for adsorption of these hydroquinone on ppy in phase gas and water solvent at B3LYP/6-31+G (d,p) and WB97XD/6-31+G(d,p) level of theory.

System	$E_{(HOMO)}(eV)$	$E_{(LUMO)}(eV)$	$E_g(eV)$	$\mu_D(Debye)$	$E_{ads}(\frac{kJ}{mol})$
hydroquinone	-5.819	-0.621	5.197	0.001	-
hydroquinonesw	-5.921	-0.681	5.239	0.0007	-
hydroquinonew	-7.741	1.297	9.038	0.0009	-
hydroquinonesww	-7.867	1.215	9.082	0.0003	-
Ppy	-4.804	-0.552	4.252	2.138	-
Ppysw	-4.844	-0.729	4.114	2.671	-
Ppyw	-6.702	1.409	8.111	2.299	-
Ppysww	-6.739	1.170	7.909	2.847	-
hydroquinone-ppy	-4.873	-0.597	4.275	2.453	-16.829
hydroquinone-ppysw	-4.744	-0.741	4.002	2.539	-2.373
hydroquinone-ppyw	-6.791	1.242	8.034	2.592	-35.939
hydroquinone-ppysww	-6.703	1.176	7.879	2.284	-25.013

3.8. Reactivity parameters

In this study, reactivity parameters including hardness (η), chemical potential (μ), softness (σ) and electrophilicity (ω) were also investigated. Chemical potential is a measure of the stability of a system and indicates the degree to which the system tends to remain in that state. The standard definition of chemical potential for a particle is defined as the change in Gibbs free energy relative to its mole. But it is shown that for an N electron system with total electron energy E and an external potential V (r) the chemical potential is as follows.

$$\mu = (\frac{\partial E}{\partial N})_{V(r)} \qquad (7)$$

Hardness is a quantity that depends on the charge and polarizability of the system. Polarization includes the concept of the excitability of electrons and orbital and energy changes. By these definitions, hardness seems to be related to electronic energy. This concept was introduced by Pearson

$$\eta = -(\frac{\partial^2 E}{\partial N^2})_{V(r)} = -(\frac{\partial \mu}{\partial N})_{V(r)} \qquad (8)$$

Kopman's theory, which is an approximate theory, calculates chemical potential and hardness as follows.

$$\mu = -\frac{(\mathrm{IP} + \mathrm{EA})}{2} = \frac{(\mathrm{E}_{LUMO} + \mathrm{E}_{HOMO})}{2}$$

$$\eta = \frac{(\mathrm{IP} - \mathrm{EA})}{2} = \frac{(\mathrm{E}_{LUMO} - \mathrm{E}_{HOMO})}{2}$$

That IP ionization energy is approximately equal to $-E_{HOMO}$ - and EA is electron-affinity energy and approximately equal to $-E_{LUMO}$. They introduced a quantity called electrophilicity, which is a measure of the tendency of a compound to pull an electron cloud from the environment toward it. The exchange-correlation function of the wb97xd has more hardness, which is in agreement with the less dipole moment. For the wb97xd functional, the electrophilicity values are lower, which is in agreement with the negative chemical potential and more hardness.

Table 2. Reactivity parameters include hardness (η), chemical potential (μ), softness (σ) and electrophilicity (ω) for adsorbate, ppy adsorbent, and adsorption this adsorbate on ppy. Calculated charge transfer by Mulliken charge analysis ($Q_{mulliken}$) and natural population analysis (Q_{NBO}) and intermolecular distance for adsorption hydroquinone on ppy at B3LYP/6-31+G (d,p) and WB97XD/6-31+G (d,p) level of theory.

System	$\eta(eV)$	$\mu(eV)$	$\sigma(eV^{-1})$	$\omega(eV)$	$d(A^{\circ})$	$Q_{NBO}(e)$	$Q_{mulliken}(e)$
hydroquinone	2.598	-3.220	0.384	1.995	-	-	-
hydroquinonesw	2.619	-3.301	0.381	2.080	-	-	-
hydroquinonew	4.519	-3.222	0.221	1.148	-	-	-
hydroquinonesw	4.541	-3.326	0.220	1.218	-	-	-
Ppy	2.126	-2.678	0.470	1.686	-	-	-
Ppysw	2.057	-2.786	0.486	1.886	-	-	-
Ppyw	4.055	-2.644	0.246	0.861	-	-	-
Ppysww	3.954	-2.784	0.252	0.980	-	-	-
hydroquinone-ppy	2.137	-2.735	0.467	1.750	2.06	+0.002	+0.011
hydroquinone-ppysw	2.001	-2.742	0.499	1.878	2.06	+0.021	-0.028
hydroquinone-ppyw	4.016	-2.774	0.249	0.958	1.93	+0.017	-0.025
hydroquinone-ppysww	3.939	-2.763	0.253	0.969	1.97	+0.026	+0.026

4. Conclusion

The calculations show that the WB97XD correlation-exchange function has more negative absorption energy than B3LYP, which could be related to the involvement of the dispersion

forces in this correlation-exchange function. The more negative absorption energy almost always increases the bandgap and this leads to the stability of the system.

Acknowledgment

The author appreciates the chemistry department of the Sharif University of Technology.

References:

[1] G. D. Sheng, D. D. Shao, X .M. Ren, X. Q. Wang, J. X. Li, Y. X. Chen, X. K. Wang, *J. Hazard. Mater*. 178(2010) 505-516.

[2] M. Watkins, N. Sizochenko, Q. Moore, M. Golebiowski, D. Leszczynska, J. Leszczynski, *J. Mol. Model.* 39(2017) 234-241.

[3] S. Suresh, V. C. Srivastava, I. M. Mishra, , *J. Chem. Eng. Data*. 56(2011) 811–818.

[4] S. H. Lin, R. S. Juang, , *J. Environ. Manage*. 90(2009) 1336-1349.

[5] R. Hu, S. Dai, D. Shao, A. Alsaedi, B. Ahmad, Xia. Wang, , *J. Mol. Liq*. 203(2015) 80-89.

[6] S. Suresha, V. C. Srivastavaa, I. M. Mishra, , *Chem. Eng. J.* 171(2011) 997–1003.

[7] S. Suresh, V. C. Srivastava, I. M. Mishra, , *J. Chem. Eng. Data*. 56(2011) 811–818.

[8] ZH. Dan, J. Haifeng, ZH. Huiying, Q. Jishi, Y. Xiaojun, DU. Qingyuan, CH. Liyue, , *Chin. J. Oceanol. Limn*. 36(2018) 726-737.

[9] J. M. G. Hernandez, G. H. Cocoletzi, E. Ch. Anota, *J. Mol. Model*. 18(2012) 137–144.

[10] S. Ghezali, A. M. Benzerdjeb, , *Aceh Int. J. Sci. Technol*. 6(2017) 141-152.

[11] M. Altarawneh, M. W. Radny, Ph. V. Smith, J. C. Mackie, E. M. Kennedy, B. Z. Dlugogorski, *Appl. Surf. Sci*. 254(2008) 4218-4224.

[12] L. M. Cam, L. V. Khu, N. N. Ha, , *J. Mol. Model*. 19(2013) 4395-4402.

[13] Z. Gh. Nezam Abadee , M. Hekmati, M. D. Ganji, *J. Mol. Liq*. 286(2019).

[14] S. Gueddida, S. Lebegue, M. Badawi, , *J. Phys. Chem. C*. 124(2020) 20262-20269.

[15] F. Maldonado, L. Villamagua, R. Rivera, , *J. Phys. Chem. C*. 123(2019) 12296-12304.

[16] D. Wei, Ch. Zhao, A. Khan, L. Sun, Y. Ji, Y. Ai, X. Wang, , *Chem. Eng. Sci*. 375(2019).

[17] N. Aarab, M. Laabd, H. Eljazouli, R. Lakhmiri, H. Kabli, A. Albourine, , *Int. J. Ind. Chem*. 10(2019) 269–279.

[18] R. Hu, S. Dai, D. Shao, A. Alsaedi, B. Ahmad, X. Wang, *J. Mol. Liq*. 203(2015) 80-89.

[19] A. Sh. Rad, N. Nasimi, M. Jafari, D. Sadeghi Shabestari, E. Gerami, , *J. Sens. Actuators B Chem*. 220(2015) 641-651.

[20] N. Aarab, A. Hsini, M. Laabd, A. Essekri, T. Laktif, M. A. Haki, R. Lakhmiri, A. Albourine, , *Mater. Today*. 22(2020) 100-103.

[21] M. Laabd, A. E. Jaouhari, M. Bazzaoui. A. Albourine, H. E. Jazouli, *J. Polym. Environ*. 25(2017) 359-369.

[22] M. Laabd, A. Hallaoui, N. Aarb, A. Essekri, H. Eljazouli, R. Lakhmiri, A. Albourine, , *Fiber Polym*. 20(2019) 896-905.

[23] A. Sh. Rad, S. Gh. Ateni, H. Tayebi, P. Valipour, V. P. Foukolaei, *J. Sulphur Chem.* 37(2016) 622-631.

[24] Nouh Aarab, A. Hsini, A. Essekri, M. Laabd, R. Lakhmiri, A. Albourine, *Groundw. Sustain. Dev*. 11(2020).

[25] S. Abdi, M. Nasiri, A. Mesbahi, M. H. Khani, *J. Hazard. Mater*. 332(2017) 132-139.

[26] M. Laabd, L. Atourki, H. Chafai, M. Bazzaoui, M. Elamine, A. Albourine, *J. Dispers. Sci. Technol.* 38(2017) 1227-1233.

[27] H. Sajid, T. Mahmood, Kh. Ayub, *Synth. MeT*. 235(2018) 49–60.

[28] Y. Xu, J. Chen, R. Chen, P. Yu, Sh. Guo, X. Wang, *Water Res*. 160(2019) 148-157.

[29] H. Chafai, M. Laabd, S. Elbariji, M. Bazzaoui, A. Albourine, *J. Dispers. Sci. Technol*. 38(2017) 832-836.

[30] J. Chen, L. Zhang, J. Zhu, N. Wang, J. Feng, W. Yan, *Appl. Surf. Sci*. 459(2018) 318-326.

[31] N. Setoodeh, P. Darvishi, F. Esmaeilzadeh, *J. Dispers. Sci. Technol*. 39(2018) 578-588.

[32] S. A. Ali Shah, M. Firlak, S. R. Berrow, N. R. Halcovitch, S. J. Baldock, B. M. Yousafzai, R. M. Hathout, J. G. Hardy, *materials*. 11(2018).

[33] S. M. Unni, V. M. Dhavale, V. K. Pillai, S. Kurungo, *J. Phys. Chem*. 114(2010) 14654–14661.

[34] A. Kannan, S. Radhakrishnan, *Mater. Today. Commun*. 25(2020).

[35] R. H. Hertwig, W. Koch, *Chem. Phys. Lett*. 268(1997) 345-351.

[36] J. D. Chaia, M. H. Gordon, *J. Chem. Phys*. 128(2008).

[37] J. D. Chai, M. H. Gordon, *Phys. Chem. Chem. Phys*. 10(2008) 6615–6620.

[38] R. G. Parr, Laszlo, V. Szentpaly, Sh. Liu, *J. Am. Chem. Soc*. 121(1999) 1922-1924.

[39] R. P. Iczkowski, J. L. Margrave. *J. Am. Chem. Soc*. 83(1961) 3547-3551.

[40] R. G. Parr, R. A. Donnelly, M. Levy, W. E. Palke, *J. Chem. Phys*. 68(1978).

[41] R. G. Parr, R. G. Pearson, *J. Am. Chem. Soc*. 105(1983) 7512-7516.

[42] V. T. Koopmans, *physica*. 1(1934) 104-113.

[43] P. Weiner, R. Langridge, J. Blaney, R. Schaefer, P. Kollman, *Proc. Natl. Acad. Sci. USA.* 79(1982) 3754-3758.

[44] E. D. Glendening, C. R. Landis, F. Weinhold, *Comput Mol Sci*. 2(2012) 1–42.

[45] W. Wang, F. M. Izrailev, G. Casati, *Phys. Rev. E*. 57(1998) 323-339.

[46] C. A. Coulson, G. S. Rashbrooke, *Math. Proc. Camb. Philos. Soc*. 36(1940) 193-200.

[47] E. Pastorczaka, C. Corminboeu, *Chem. Phys.* 146(2017).